ISSN 1674-1056
http://cpb.iphy.ac.cn
http://iopscience.iop.org/cpb
中国物理 B
Chinese Physics
中国物理 Chinese Physics B

Studying the charge carrier properties in $CuInS_2$ films via femtosecond transient absorption and nanosecond transient photocurrents

Mingrui Tan(谭铭瑞), Qinghui Liu(刘庆辉), Ning Sui(隋宁), Zhihui Kang(康智慧), Liquan Zhang(张里荃), Hanzhuang Zhang(张汉壮), Wenquan Wang(王文全), Qiang Zhou(周强), Yinghui Wang(王英惠)

Citation: Chin. Phys. B . 2019, 28(5): 056106. **doi:** 10.1088/1674-1056/28/5/056106
Journal homepage: http://cpb.iphy.ac.cn; http://iopscience.iop.org/cpb

What follows is a list of articles you may be interested in

Influences of total ionizing dose on single event effect sensitivity in floating gate cells

Ya-Nan Yin(殷亚楠), Jie Liu(刘杰), Qing-Gang Ji(姬庆刚), Pei-Xiong Zhao(赵培雄), Tian-Qi Liu(刘天奇), Bing Ye(叶兵), Jie Luo(罗捷), You-Mei Sun(孙友梅), Ming-Dong Hou(侯明东)
Chin. Phys. B . 2018, 27(8): 086103. **doi:** 10.1088/1674-1056/27/8/086103

Investigation of flux dependent sensitivity on single event effect in memory devices

Jie Luo(罗捷), Tie-shan Wang(王铁山), Dong-qing Li(李东青), Tian-qi Liu(刘天奇), Ming-dong Hou(侯明东), You-mei Sun(孙友梅), Jing-lai Duan(段敬来), Hui-jun Yao(姚会军), Kai Xi(习凯), Bing Ye(叶兵), Jie Liu(刘杰)
Chin. Phys. B . 2018, 27(7): 076101. **doi:** 10.1088/1674-1056/27/7/076101

Non-monotonic dependence of current upon i-width in silicon p-i-n diodes

Zheng-Peng Pang(庞正鹏), Xin Wang(王欣), Jian Chen(陈健), Pan Yang(杨盼), Yang Zhang(张洋), Yong-Hui Tian(田永辉), Jian-Hong Yang(杨建红)
Chin. Phys. B . 2018, 27(6): 066106. **doi:** 10.1088/1674-1056/27/6/066106

Ab-initio investigation of $AGeO_3$ (*A*=Ca, Sr) compounds via Tran–Blaha-modified Becke–Johnson exchange potential

Rasul Bakhsh Behram, M A Iqbal, Muhammad Rashid, M Atif Sattar, Asif Mahmood, Shahid M Ramay
Chin. Phys. B . 2017, 26(11): 116103. **doi:** 10.1088/1674-1056/26/11/116103

Slip on the surface of silicon wafers under laser irradiation:Scale effect

Zhi-Chao Jia(贾志超), Ze-Wen Li(李泽文), Jie Zhou(周洁), Xiao-Wu Ni(倪晓武)
Chin. Phys. B . 2017, 26(11): 116102. **doi:** 10.1088/1674-1056/26/11/116102

Studying the charge carrier properties in $CuInS_2$ films via femtosecond transient absorption and nanosecond transient photocurrents*

Mingrui Tan(谭铭瑞)[1], Qinghui Liu(刘庆辉)[1], Ning Sui(隋宁)[1], Zhihui Kang(康智慧)[1], Liquan Zhang(张里荃)[1,†], Hanzhuang Zhang(张汉壮)[1,‡], Wenquan Wang(王文全)[1], Qiang Zhou(周强)[2], and Yinghui Wang(王英惠)[1]

[1] *Femtosecond Laser Laboratory, Key Laboratory of Physics and Technology for Advanced Batteries, College of Physics, Jilin University, Changchun* 130012, *China*

[2] *State Key Laboratory of Superhard Materials, College of Physics, Jilin University, Changchun* 130012, *China*

(Received 1 November 2018; revised manuscript received 20 March 2019; published online 22 April 2019)

The carrier behavior in $CuInS_2$ thin films at femtosecond and microsecond time scales is discussed in detail. Transient absorption data suggests that the photo-generated carriers relax rapidly accompanied by a change in energy. The photo-generated charge carriers are extracted by a bias electric field E in the nanosecond transient photocurrent system. An applied E improves the efficiency of photon conversion to charge carriers and enhances the velocity of the extracted charge carriers. In addition, there exists a threshold of illumination intensity in the extraction process of charge carriers in the $CuInS_2$ thin film, above which carrier recombination occurs. The corresponding loss further increases with illumination intensity and the recombination rate is almost independent of E. Our results provide useful insights into the characteristics of carriers in the $CuInS_2$ thin film and are important for the operation of optoelectronic devices realized with these films.

Keywords: semiconductor film, carrier dynamics, transient absorption, transient photocurrent

PACS: 61.82.Fk, 68.35.bg, 73.50.Gr **DOI:** 10.1088/1674-1056/28/5/056106

1. Introduction

Metal sulfide thin films are bulk semiconductors that have attracted much attention recently because of their excellent properties. Examples include CuS,[1] Cu_2S,[2] ZnS,[3] CdS,[4] SnS,[5] FeS_2,[6] Sb_2S_3,[7] $CuAlS_2$,[8] Cu_2BaS_2,[9] $CuInS_2$,[10] and Cu_2ZnSnS_4.[11] The synthesis process can be tuned and easily controlled,[12,13] and their performance is better than nanocrystal films. This is influenced by the surface ligands of the nanocrystal.[14] Therefore, metal sulfide thin films are promising candidates in optoelectronic devices such as photovoltaic and photoconductive devices.

$CuInS_2$ is a representative metal sulfide with many attractive attributes, such as optimal bandgaps,[15] a large absorption coefficient,[16] and low toxicity.[17] To develop optoelectronic devices based on $CuInS_2$ thin films, it is necessary to study the charge carrier generation, transportation, and recombination mechanisms. However, the understanding of the carrier dynamics in the $CuInS_2$ thin films remains limited. These materials have an amorphous structure,[12,13] and the corresponding photo-physical properties are different from nanocrystals. In addition, the carrier behavior in the inorganic semiconductor film is affected by many factors. Due to these complexities, a single test method is insufficient to analyze this process.

Here, we have simultaneously applied femtosecond transient absorption and nanosecond transient photocurrent to probe the carrier behavior in the $CuInS_2$ thin films. The results provide a better understanding of carrier behavior in the $CuInS_2$ film and aid in determining the intrinsic physical characteristics that are independent of the external condition.

2. Experimental methods

$CuInS_2$ thin films were synthesized as described in the previous report.[13] 2 mmol S powder, 2 mL 1-butylamine, 0.6 mL thioglycolic acid, 1 mmol $Cu(Ac)_2$, and 1 mmol $In(Ac)_3$ were added into 5 mL ethanol under room temperature to form stable $CuInS_2$ solution. The films were fabricated by spin-coating the solution on indium tin oxide (ITO) and quartz glass substrates followed by 350 °C sintering for 3 min, which was repeated several times. The device structure was designed by following a planar ITO/$CuInS_2$ film/Al structure as previously reported.[18] The nominal device area was 4 mm^2, which was defined by the overlap between the anode and cathode. An ohmic contact was formed between ITO anode and $CuInS_2$ film,[19] whereas the contact between $CuInS_2$ film and the Al cathode was a Schottky contact.[20] Steady-state absorption measurements were performed with an ultraviolet–visible (UV–Vis) absorption spectrometer (Purkinje, TU-1810 PC). The crystallographic information on the samples was deter-

*Project supported by the National Natural Science Foundation of China (Grant Nos. 21573094, 51502109, 11774122, 11574112, and 11474131), the National Found for Fostering Talents of Basic Science, China (Grant No. J1103202), and the China Scholarship Council (CSC) obtained during the visit of Ning Sui to MPIA (Grant No. 201706175038).

†Corresponding author. E-mail: zhanglq@jlu.edu.cn

‡Corresponding author. E-mail: zhanghz@jlu.edu.cn

© 2019 Chinese Physical Society and IOP Publishing Ltd

mined by a Bruker D8 advance x-ray diffractometer (Cu $K\alpha$, $\lambda = 1.5418$ Å, 40 kV, and 30 mA). The femtosecond transient absorption (TA) technique has been described in a prior report.[21]

The nanosecond transient photocurrent was composed of a nanosecond laser (Quantel, QS450-2W3W) and oscilloscope (Tektronix TDS 3032C). To ensure uniform distribution of the photo-generated carriers, we used an optical parametric oscillator (OPO) module (MagicPRISM VIS) to obtain the excitation light pulse with a wavelength of 680 nm, where the absorption value of the sample was approximately 0.33.

3. Results and discussion

Figure 1(a) shows the absorption spectra of the $CuInS_2$ thin film with a band-edge located near 830 nm. The spectra show no obvious features in the frequency domain.[22] The cross-sectional scanning electron microscope (SEM) image in Fig. 1(a) shows a film thickness of 300 nm. To verify the phase purity, x-ray diffraction (XRD) is performed and a wurtzite structure[23] is obtained for the $CuInS_2$ thin film, as shown in Fig. 1(b).

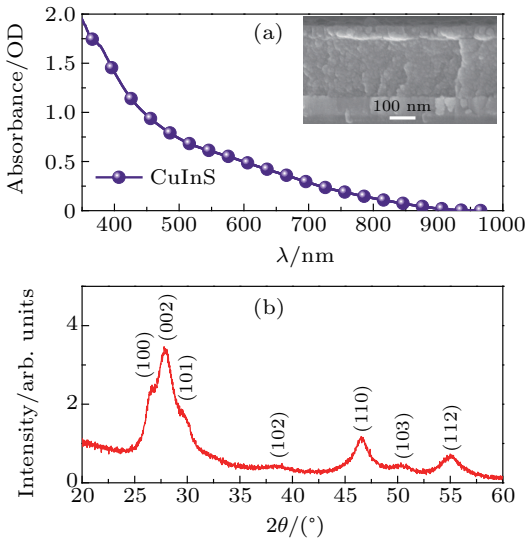


Fig. 1. (a) The absorption spectrum of the $CuInS_2$ film. (b) The XRD patterns of the $CuInS_2$ thin films. Inset: SEM of the $CuInS_2$ film.

Figure 2(a) shows a map of transient absorption data of the $CuInS_2$ thin film excited at 400 nm. Comparing with the steady state absorption, there is a positive signal from 550 nm to 750 nm and a minor negative signal above 550 nm, corresponding to the excited state absorption (ESA) and the ground bleaching, respectively. The ESA peak is gradually redshifted, and its intensity decreases with time. This redshift is attributed to the change in carrier energy, whereas the intensity decrease is assigned to population relaxation, diffusion, and recombination of photo-generated carriers.[24,25]

Figure 2(a) shows that the final energy of the photo-generated carrier is about 1.7 eV, which suggests that the energy of the photo-generated carrier varies about 0.2 eV during relaxation. To further analyze the carrier properties, the time-dependent variance of carrier energy (E–T curve) and intensity (I–T curve) of ESA are generated, as shown in Fig. 2(b). The E–T dynamics decay rapidly versus I–T. We have employed a multi-exponential function to analyze the curves and determine their average decay lifetime. The fitted results from complex and non-exponential decay behaviors are shown in Fig. 2(b), where the lifetimes of E–T and I–T are determined to be 2.00 ps and 1.49 ps, respectively.

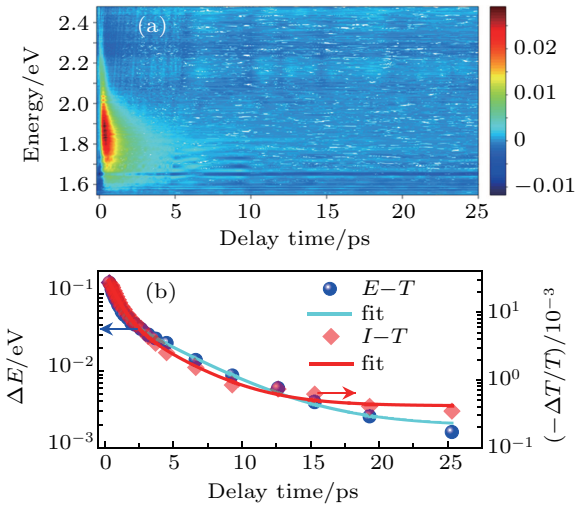


Fig. 2. (a) Map of transient absorption data. (b) Time-dependent carrier energy and population.

Next, the nanosecond transient photocurrent[26] method is employed to further investigate the dynamic behavior of the carriers. A bias electric field applied to the $CuInS_2$ film is used to extract the carriers. The illumination intensity-dependent photocurrent transients are shown in Fig. 3(a). The amplitude of the photocurrent increases almost linearly with the light intensity, as evidenced from the inset in Fig. 3(a). A saturation feature is obtained when the light is stronger than 0.56 μJ·mm^{-2}. This suggests that the loss of the carrier originating from the light intensity could be ignored with weak illumination.

Figure 3(b) shows the electric field-dependent current density j_0 when the illumination is 0.17 μJ·mm^{-2}. j_0 is detected by the oscilloscope, even though there is no bias electric field E on the $CuInS_2$ film. This suggests that j_0 mainly originates from temperature-induced carrier diffusion.[27] Under an applied E, j_0 is enhanced due to mobility of the photo-generated charge carriers, as shown in Fig. 3(b). Notably, both decay curves of j_0 in Figs. 3(a) and 3(b) show a non-exponential behavior because the diffusion, migration, and recombination of carriers participate in the relaxation behavior of j_0. In addition, the concentration of extracted charge carriers N also increases with j_0, as seen in the time integrated

plots in Figs. 3(a) and 3(b). The evolution of N under different E values is given in Fig. 3(c) at the light intensity of 0.17 μJ·mm^{-2} and 5.31 μJ·mm^{-2} , respectively. Both the corresponding values of N gradually increase with E and reach saturation at each irradiation intensity. The number of photo-generated carriers in the film is constant under a fixed illumination intensity, and can be fully extracted when E is sufficiently high. The photo-generated carriers recombine under stronger light. However, the E-dependent evolution of N at an illumination intensity of 5.31 μJ·mm^{-2} is similar to that of 0.17 μJ·mm^{-2}, suggesting that it is insensitive to the number of charge carriers in the film.

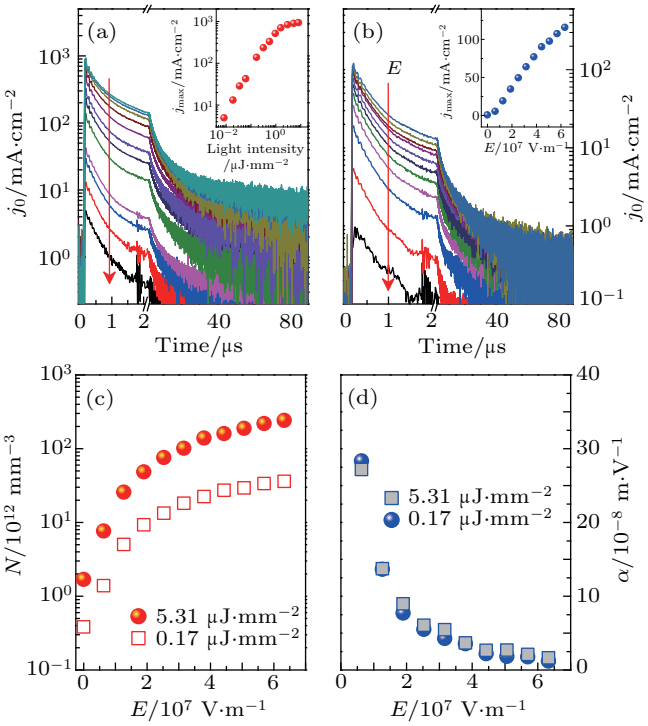


Fig. 3. (a) The illumination intensity-dependent and (b) applied electric field-dependent transient photocurrent curves. Insets: corresponding maximum (a) illumination intensity-dependent and (b) applied electric field-dependent transient photocurrent. (c) The concentration of extracted charge carriers and (d) α versus applied electric field measured under different illumination intensities (0.17 μJ·mm^{-2} and 5.31 μJ·mm^{-2}), respectively. The illumination intensities are 8.25, 5.31, 2.99, 1.61, 0.96, 0.56, 0.32, 0.17, 0.062, 0.035, 0.019, and 0.0083 (in units of μJ·mm^{-2}) in (a) and 0.17 μJ·mm^{-2} in (b). The applied electric fields are 6.33×10^7 V·m^{-1} in (a) and 6.33×10^7, 5.70×10^7, 5.06×10^7, 4.43×10^7, 3.80×10^7, 3.16×10^7, 2.53×10^7, 1.90×10^7, 1.27×10^7, and 0.63×10^7 (in units of V·m^{-1}) in (b).

To further discuss the role of E in the nanosecond transient photocurrent test, we define $\alpha = \mathrm{d}(N)/N\mathrm{d}(E)$ as the fraction of charge carriers driven by E, as shown in Fig. 3(d) as a function of E. The α gradually decreases with E and is almost zero when E increases to 6.33×10^7 V·m^{-1}, which implies that the photo-generated charge carriers in the $CuInS_2$ film may be extracted more effectively under a higher electric field. However, α only undergoes a minor change with illumination intensity, which is likely due to photo-generated carrier recombination.

Figure 4(a) further shows the evolution of the photo-generated charge carriers versus different absorbed photon numbers (APNs) under an E of 1.27×10^7 V·m^{-1} and 6.33×10^7 V·m^{-1}, respectively. The N linearly increases with APN when the APN is lower than 1.79×10^{14} mm^{-3}. At higher values, the variance of N induced by APN becomes smaller and eventually saturates as APN increases further. This is likely to be due to incomplete extraction of photo-generated charge carriers in the $CuInS_2$ thin film, as some of them may be lost due to recombination or collision annihilation.

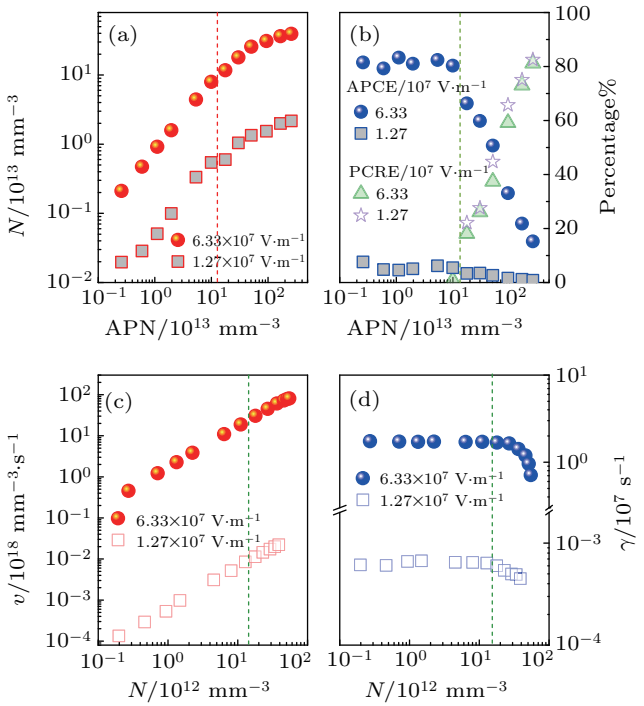


Fig. 4. APN-dependent (a) N and (b) APCE and PCRE under different applied electric fields (6.33×10^7 V·m^{-1} and 1.27×10^7 V·m^{-1}). (c) The extracted velocity of charge carrier v and (d) γ versus N under an applied electric field of 6.33×10^7 V·m^{-1} and 1.27×10^7 V·m^{-1}, respectively.

The evolution of N at different APN values is similar as E increases from 1.27×10^7 V·m^{-1} to 6.33×10^7 V·m^{-1}, suggesting that this phenomenon is insensitive to E. APN-dependent absorbed photon-to-electron conversion efficiency (APCE) is shown in Fig. 4(b). At a fixed E of 6.33×10^7 V·m^{-1}, the initial APCE is close to 81% and does not vary with APN. The APCE rapidly decreases after the APN increases to 9.92×10^{13} mm^{-3} (0.32 μJ·mm^{-2}). This can be attributed to the loss caused by carrier recombination.

We also studied the photo-generated carrier recombination efficiency (PCRE) given by (81%−APCE)/81%; the results are shown in Fig. 4(b) with E of 6.33×10^7 V·m^{-1}. The PCRE gradually increases with APN values over 9.92×10^{13} mm^{-3}, indicating that the loss of carriers is due to the carrier–carrier collision at high carrier concentrations. The APCE is under 10% when E decreases to 1.27×10^7 V·m^{-1}. The APCE is strongly dependent on E because the value of

E determines the number of extracted free charge carriers. The PCRE at 1.27×10^7 V·m^{-1} is similar to the value at 6.33×10^7 V·m^{-1}, as shown in Fig. 4(b). This suggests that the recombination process in the film is affected by the APN but not by E.

The lifetime τ_e of j_0 corresponds to the time when j_0 decreases to the $1/e$ of its amplitude at $t = 0$. We also define $v = N_e/t_e$ to estimate the extraction velocity of charge carriers, where N_e is the number of extracted charge carriers during the period of τ_e. The v gradually increases with E and N, as shown in Fig. 4(c). However, the evolution of v at 6.33×10^7 V·m^{-1} is similar to that at 1.27×10^7 V·m^{-1}. To ascertain the reason behind the similarity of v at different E values, we define $\gamma = \mathrm{d}(v)/\mathrm{d}(N)$, as shown in Fig. 4(d). The γ is almost independent of N below 1.79×10^{13} mm^{-3}, which implies that the carrier mobility during that process is constant. When N is higher than 1.79×10^{13} mm^{-3}, γ begins to decrease with N at fixed E, suggesting that the variance of v induced by N gradually decreases. In this situation, migration plays a negative role in the extraction process of charge carriers because the carriers in the $CuInS_2$ film are congested, which decelerates directional movement of carriers and leads to carrier–carrier collisions. The evolution of γ at 1.27×10^7 V·m^{-1} is similar to that at 6.33×10^7 V·m^{-1}, suggesting that the evolution of γ at different N values is almost insensitive to E, even though it determines the amplitude of γ.

4. Conclusion and perspectives

In summary, we have investigated the carrier kinetic behavior in $CuInS_2$ films based on femtosecond transient absorption and nanosecond transient photocurrent methods. Femtosecond transient absorption confirms that the carrier relaxation is complex and accompanied by a change of carrier energy. The nanosecond transient photocurrent analyzes the role of bias electric field and illumination intensity in the extraction process. Carrier recombination occurs when the illumination is higher than a certain threshold. The corresponding loss further increases with the illumination intensity. The recombination percentage is almost independent of the bias electric field. The carriers are extracted by the bias electric field, which improves the efficiency of photon conversion to charge carriers and enhances the velocity of the extracted charge carriers. These results provide insights into the dynamic behavior of charge carriers in inorganic thin films, which is essential for the development of optoelectronic devices.

References

[1] Lu Y J, Meng X, Yi G W and Jia J H 2011 *J. Colloid. Interface. Sci.* **356** 726
[2] Wu Y, Wadia C, Ma W L, Sadtler B and Alivisatos A P 2008 *Nano Lett.* **8** 2551
[3] Elidrissi B, Addou M, Regragui M, Bougrine A, Akchouane A and Bernede J C 2001 *Mater. Chem. Phys.* **68** 175
[4] Voss C, Subramanian S and Chang C H 2004 *J. Appl. Phys.* **96** 5819
[5] Parkin I P, Price L S, Hibbert T G and Molloy K C 2001 *J. Mater. Chem.* **11** 1486
[6] Berry N, Cheng M, Perkins C L, Limpinsel M, Hemminger J C and Law M 2012 *Adv. Energy Mater.* **2** 1124
[7] Messina S, Nair M T S and Nair P K 2007 *Thin Solid Films* **515** 5777
[8] Caglar M, Ilican S and Caglar Y 2008 *Opt. Commun.* **281** 1615
[9] Wang Y M, Liu M L, Huang F Q, Chen L D, Li H L, Lin X P, Wang W D and Xia Y J 2007 *Chem. Mater.* **19** 3102
[10] Li L, Coates N and Moses D 2010 *J. Am. Chem. Soc.* **132** 22
[11] Steinhagen C, Panthani M G, Akhavan V, Goodfellow B, Koo B and Korgel B A 2009 *J. Am. Chem. Soc.* **131** 12554
[12] Tian Q W, Wang G, Zhao W E, Chen Y Y, Yang Y C, Huang L J and Pan D C 2014 *Chem. Mater.* **26** 3098
[13] Zhao W, Wang G, Tian Q, Yang Y, Huang L and Pan D 2014 *ACS Appl. Mater. Interfaces* **6** 12650
[14] Wang G, Wang S, Cui Y and Pan D 2012 *Chem. Mater.* **24** 3993
[15] Sheng X, Wang L, Chang L, Luo Y, Zhang H, Wang J and Yang D 2012 *Chem. Commun.* **48** 4746
[16] Theresa J T, Meril M, Sudha K C, Vijayakumar K P, Abe T and Kashiwaba Y 2005 *Sol. Energy Mater. Sol. Cells* **89** 27
[17] Jia Y, Wang H, Yan Z, Deng L, Dong H, Ma N and Sun D 2016 *RSC Adv.* **6** 93303
[18] Bi K, Sui N, Zhang L Q, Wang Y H, Liu Q H, Tan M R and Zhang H Z 2016 *J. Nanopart. Res.* **18** 367
[19] Kijatkina O, Krunks M, Mere A, Mahrov B and Dloczik L 2003 *Thin Solid Films* **431–432** 105
[20] Mere A, Kijatkina O, Rebane H, Krustok J and Krunks M 2003 *J. Phys. Chem. Solids* **64** 2025
[21] Liu Q H, Wang Y H, Sui N, Wang Y T, Chi X C, Wang Q Q, Chen Y, Ji W Y, Zou L and Zhuang H Z 2016 *Sci. Rep.* **6** 29442
[22] Lu X T, Zhuang Z B, Peng Q and Li Y D 2011 *CrystEngComm* **13** 4039
[23] Hao Z M, Cui Y and Wang G 2015 *Mater. Lett.* **146** 77
[24] Yamada Y, Yasuda H, Tayagaki T and Kanemitsu Y 2009 *Phys. Rev. Lett.* **102** 247401
[25] Yasuda H and Kanemitsu Y 2008 *Phys. Rev. B* **77** 193202
[26] Soci C, Moses D, Xu Q H and Heeger A J 2005 *Phys. Rev. B* **72** 245204
[27] Schultes F J, Christian T, Jones-Albertus R, Pickett E, Alberi K, Fluegel B, Liu T, Misra P, Sukiasyan A, Yuen H and Haegel N M 2013 *Appl. Phys. Lett.* **103** 242106